Theoretical and Experimental Study of Valence-Shell Ionization Spectra of Guanine†

Irina L. Zaytseva,‡ Alexander B. Trofimov,‡,§ Jochen Schirmer,|| Oksana Plekan,⊥,# Vitaliy Feyer,⊥ Robert Richter,⊥ Marcello Coreno,▽ and Kevin C. Prince*,⊥,¶

Laboratory of Quantum Chemistry, Irkutsk State University, 664003 Irkutsk, Russia, Favorsky Institute of Chemistry, SB RAS, 664033 Irkutsk, Russia, Theoretische Chemie, Physikalisch-Chemisches Institut, Universität Heidelberg, Im Neuenheimer Feld 229, D-69120 Heidelberg, Germany, Sincrotrone Trieste, in Area Science Park, I-34149 Basovizza (Trieste), Italy, CNR-IMIP, c/o GasPhase@Elettra (Trieste), Montelibretti (Rome), I-00016 Italy, and Laboratorio Nazionale TASC, INFM-CNR, 34149 Trieste, Italy

Received: June 5, 2009; Revised Manuscript Received: August 21, 2009

The full valence-shell ionization spectra of the four most stable guanine tautomers were studied theoretically. The third-order algebraic-diagrammatic construction (ADC(3)) method for the one-particle Green's function was used to calculate the energies and relative intensities of the vertical ionization transitions. For low-lying transitions, the influence of planar and nonplanar guanine configurations on the ionization energies, as well as the convergence of the results with respect to basis set was studied at the level of the outer-valence Green's function (OVGF) approximation scheme. The results of the calculations were used to interpret recent synchrotron radiation valence-shell photoionization spectra of guanine in the gas phase under thermal equilibrium conditions. The photoelectron spectrum was modeled by summing individual tautomer spectra weighted by Boltzmann population ratios (BPR) of tautomers from our previous high-level ab initio thermochemical calculations. The theoretical spectra are in good agreement with the experimental results, providing assignments of most observed structures and offering insight into tautomerism of guanine in the gas phase. The first six molecular orbitals give rise to single-hole states with a binding energy of about 7−12 eV. At higher binding energy the spectral features are mainly due to satellite states.

I. Introduction

Guanine is a molecule that exists in several tautomeric forms at laboratory temperatures[1] and is of great importance as one of the building blocks of life. A fundamental property of molecules is their valence electron spectrum, because it allows an understanding of how the molecule is bonded. To our knowledge, there have been only few experimental studies of the outer valence region of guanine.[2−5] In the past the photoelectron spectra of guanine tautomers and its derivatives in the energy range below 14 eV were exhaustively studied theoretically by Dolgounicheva et al.[6] using the partial third-order method (P3).[7] More recently, valence ionization of guanine tautomers **1** and **2** (Figure 1) were investigated by Jones et al.[8] using density functional theory (DFT), the statistical average of model orbital potentials (SAOP) method,[9] and outer valence Green's function (OVGF) theory.[10,11] In the present work, we report detailed calculations of the four lowest energy tautomers of guanine performed using the full third-order algebraic-diagrammatic construction [ADC(3)] method for the one-particle Green's function[10,12,13] and compare our results with new experimental data, as well as with previous theoretical calculations. The present theoretical and experimental study extends the investigation of the guanine spectrum up to an ionization energy of about 30 eV and so characterizes its entire valence region. Moreover, it allows us to identify important satellite states and search for prominent signatures of guanine tautomerism in its photoelectron spectrum.

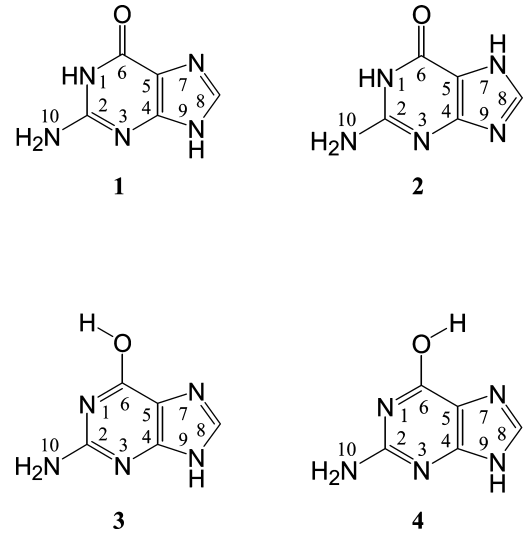

Figure 1. Schematic representation of guanine tautomers.

II. Experimental and Theoretical Methods

II.1. Theoretical Approach. Essentially the same theoretical approach as in the previous study of valence-shell ionization in cytosine, thymine, adenine,[14] and purine and pyrimidine[15] was employed. The energies and intensities of the vertical outer- and inner-valence photoelectron transitions of guanine were

† Part of the "Vincenzo Aquilanti Festschrift".
* Corresponding author. E-mail: Prince@Elettra.Trieste.It.
‡ Irkutsk State University.
§ Favorsky Institute of Chemistry.
|| Universität Heidelberg.
⊥ Sincrotrone Trieste.
Permanent address: Institute of Electron Physics, 88017 Uzhgorod, Ukraine.
▽ CNR-IMIP.
¶ INFM-CNR.

10.1021/jp905299z
Published on Web 10/02/2009

computed using the third-order algebraic-diagrammatic construction approximation scheme [ADC(3)][10,12,13] for the one-particle Green's function. The ADC(3) scheme is a direct method in which the ionization energies and the corresponding spectroscopic factors are obtained in one step as solutions of a Hermitian eigenstate problem without separate calculations for the initial and final states, which ensures a balanced description of the spectra. The resulting eigenvalues are the vertical ionization energies E_n and the components $x_p^{(n)}$ of the eigenvectors define the probability of finding the final ionic state $|\Psi_n^{N-1}\rangle$ in a pseudostate $a_p|\Psi_o^N\rangle$ produced by the sudden ejection of an electron out of the molecular orbital ϕ_p in the initial state $|\Psi_o^N\rangle$:

$$x_p^{(n)} = \langle \Psi_n^{N-1} | a_p | \Psi_o^N \rangle \quad (1)$$

As the measure of spectral intensity P_n ("pole strength") we use an approximate partial-channel cross section

$$P_n = \sigma_n \propto \sum_p \left| x_p^{(n)} \right|^2 \quad (2)$$

where the summation is performed over the whole range of available molecular orbitals (MO). The ADC(3) method combines perturbative and variational techniques in such a way that optimal balance of the accuracy and computational efficiency is achieved. In ADC(3) the ionized states are described in terms of single hole (1h) and two-hole one-particle (2h−1p) configurations, which are treated through third and first order of the many-body perturbation theory, respectively. All main effects accompanying ionization (electron correlation in the initial and final states, orbital relaxation) are accounted for in a consistent manner. This allows for a reliable description of most types of final states including those involved in the situation known as "breakdown of the one-electron picture of ionization".[16] Compared to the configuration interaction (CI) treatments of equal accuracy, the ADC(3) method has the advantage that more compact eigenstate problems have to be solved.[12,17] Moreover, ADC(3) is a so-called size-consistent method.[18] Altogether these are the essential prerequisites for a reliable description of ionization phenomena in a variety of molecular systems. The ADC(3) method has proved itself a valuable tool for interpretation of the valence-shell ionization spectra obtained using synchrotron radiation, for it is one of the few methods rendering insight into the inner-valence region of the spectra probed in this type of experiment.[14,15,19−21] The adequate treatment of the spectra is especially important for larger heterocyclic and conjugated molecules (to which classes guanine belongs) because of the relatively early onset of the "selective" breakdown regime of ionization, characterized in these compounds by strong redistribution of intensity from the inner π-type MO to various shakeup and shake-down satellite states.[19,20]

The double-ζ 6-31G basis set[22] was used in our ADC(3) calculations. This basis set is relatively compact but is sufficient for assignment of synchrotron radiation photoelectron spectra, as was confirmed by our previous ADC(3) studies of nucleobases and related molecules.[14,15,21] To assess the convergence of the outer-valence ionization energies with respect to basis set, calculations were also performed at the level of the outer-valence Green's function (OVGF) scheme[10,11] using both the 6-31G and larger 6-311++G**[23] basis sets. The OVGF scheme is theoretically less rigorous than the ADC(3) scheme, but it requires less computational effort so that larger basis sets can be employed in the calculations.

The ground-state geometrical parameters of the four most stable guanine tautomers (Figure 1) were the same as in our previous study of the core-level ionization and excitation spectra of these systems.[24] They were obtained by means of the restricted geometry optimization procedure treating the guanine tautomers as planar molecules (i.e., neglecting the out-of-plane bending of NH_2 groups). The planar structure approximation permits the use of molecular symmetry of the C_s point group, which reduces the computational effort of ADC(3) calculations and simplifies interpretation of the results. The geometry optimization was performed using density functional theory with the Becke-three-parameters-Lee−Yang−Parr (B3LYP) potential[25] and the 6-311G** basis sets[23] (see Supporting Information). The OVGF/ 6-311++G** calculations were also performed for the fully optimized nonplanar structures of the guanine tautomers, obtained in our previous work[24] at the MP2/cc-pVTZ level of theory.

The DFT/B3LYP and OVGF calculations were carried out using the GAUSSIAN package of programs.[26] The ADC(3) calculations were performed using the original code[27] linked to the GAMESS ab initio program package.[28] The frozen-core approximation was adopted in all ADC(3) and OVGF calculations, that is, the 1s orbitals were excluded from consideration. The latter approximation is also used throughout the present article for notation of guanine molecular orbitals.

The spectral envelopes were generated by convoluting the discrete transition lines with Lorentzian lines of 0.6 eV fwhm (full width at half-maximum). The widths were chosen to match the theoretical spectrum to the experiment, and are due to the convolution of experimental resolution, unresolved vibrational structure and natural lifetime widths.

The full theoretical spectrum of guanine was constructed as a sum of spectra of the individual tautomers. The Boltzmann

TABLE 1: Mulliken Atomic Population in the Most Important Outer-Valence Molecular Orbitals of Guanine 1 (in Electrons; Sum over All Atoms = 2) Calculated at the HF/6-31G Level

	population in molecular orbitals												
atom	1a″(π_1)	16a′(σ)	17a′(σ)	18a′(σ)	2a″(π_2)	3a″ (π_3)	19a′(σ)	4a″(π_4)	20a′(σ)	5a″(π_5)	21a′(σ)	6a″(π_6)	7a″(π_7)
N_1	0.40	0.14	0.06	0.06	0.29	0.07	0.05	0.03	0.18	0.89	0.03	0.05	0.01
C_2	0.31	0.17	0.02	0.01	0.19	0.16	0.08	0.0	0.02	0.0	0.04	0.0	0.10
N_3	0.23	0.30	0.07	0.0	0.01	0.18	0.96	0.39	0.11	0.18	0.39	0.12	0.30
C_4	0.23	0.24	0.11	0.04	0.14	0.02	0.07	0.19	0.0	0.09	0.14	0.01	0.23
C_5	0.16	0.06	0.07	0.25	0.10	0.06	0.10	0.01	0.19	0.0	0.14	0.41	0.51
C_6	0.16	0.09	0.32	0.16	0.02	0.51	0.0	0.0	0.05	0.04	0.03	0.0	0.01
N_7	0.06	0.09	0.06	0.37	0.17	0.01	0.59	0.26	0.13	0.08	0.86	0.46	0.13
C_8	0.06	0.22	0.03	0.56	0.27	0.0	0.03	0.19	0.01	0.10	0.05	0.0	0.37
N_9	0.18	0.29	0.07	0.04	0.62	0.04	0.05	0.0	0.01	0.0	0.07	0.83	0.01
N_{10}	0.13	0.15	0.01	0.0	0.19	0.32	0.01	0.90	0.01	0.15	0.0	0.03	0.12
O	0.07	0.07	1.14	0.17	0.02	0.63	0.0	0.03	1.25	0.46	0.22	0.08	0.20

TABLE 2: Mulliken Atomic Population in the Most Important Outer-Valence Molecular Orbitals of Guanine 2 (in Electrons; Sum over All Atoms = 2) Calculated at the HF/6-31G Level

	population in molecular orbitals												
atom	1a″(π_1)	16a′(σ)	17a′(σ)	18a′(σ)	2a″(π_2)	3a″(π_3)	19a′(σ)	4a″(π_4)	20a′(σ)	5a″(π_5)	21a′(σ)	6a″(π_6)	7a″(π_7)
N_1	0.41	0.23	0.03	0.01	0.31	0.04	0.05	0.02	0.18	0.87	0.03	0.10	0.01
C_2	0.24	0.12	0.05	0.07	0.22	0.19	0.05	0.0	0.05	0.0	0.04	0.01	0.12
N_3	0.15	0.21	0.05	0.15	0.03	0.21	0.45	0.35	0.40	0.02	0.63	0.24	0.36
C_4	0.18	0.14	0.05	0.30	0.06	0.06	0.06	0.41	0.02	0.02	0.15	0.01	0.18
C_5	0.23	0.18	0.09	0.04	0.13	0.02	0.06	0.0	0.12	0.0	0.21	0.27	0.59
C_6	0.23	0.18	0.35	0.03	0.02	0.45	0.02	0.0	0.05	0.03	0.02	0.0	0.02
N_7	0.20	0.33	0.03	0.06	0.59	0.0	0.07	0.51	0.01	0.03	0.03	0.17	0.16
C_8	0.08	0.13	0.10	0.50	0.28	0.03	0.06	0.02	0.0	0.0	0.03	0.35	0.14
N_9	0.07	0.06	0.01	0.38	0.17	0.05	0.85	0.16	0.04	0.01	0.71	0.76	0.02
N_{10}	0.09	0.10	0.03	0.06	0.18	0.30	0.0	0.53	0.02	0.52	0.0	0.06	0.18
O	0.11	0.12	1.14	0.11	0.01	0.65	0.28	0.0	1.08	0.51	0.14	0.02	0.22

population ratios (BPRs) of the tautomers **1**−**4** at the experimental temperature of 600 K were 0.246:0.354:0.213:0.158, as derived from our previous thermochemical study.[24] The theoretical intensities I in the full spectrum were defined as $I = P \times BPR$.

II.2. Experimental Section. The samples were obtained from Sigma-Aldrich with minimum purity of 99% and used without any further purification. They were evaporated from a home-built furnace at 600 K and were checked before the experiment using photoionization mass spectroscopy, to ensure that there were no effects due to thermal decomposition. The peak energies were consistent with those of Dougherty et al.[3] and Lin et al.[2] measured at 21.2 eV, but with different relative peak intensities due to different cross sections. The spectra were taken at the Gas phase Photoemission beamline, Elettra, Trieste.[29] Further details are given in ref 24.

III. Results and Discussion

It is useful to begin by describing briefly the characteristics of the outer-valence molecular orbitals of guanine tautomers. Tautomers are basically different molecules and their valence electronic structures are distinct, which should also be reflected in the corresponding valence-shell photoelectron spectra. The latter consideration does not pertain to the structures **3** and **4**, which are two rotamers of the same tautomer, differing by the orientation of OH group.

In the (planar) guanine tautomers (Figure 1), the p-type atomic orbitals of the 11 second row atoms form 11 π-type MOs (of a″ symmetry within the C_s point group). Since each of the carbon and unsubstituted nitrogen and oxygen atoms contribute one p-electron, and each of the NH, NH_2, and OH groups contribute a pair of p-electrons, there are 7 occupied π-type MOs in each tautomer. Of these MOs, 4 orbitals correspond to double bonds and the other 3 orbitals are due to the lone pairs of the NH, NH_2, and OH groups. The 4 unoccupied π MOs are the antibonding counterparts of the 4 double bond MOs. The other prominent highest occupied orbitals are σ-type MOs (of a′ symmetry) due to the lone pairs of oxygen and unsubstituted nitrogen atoms. In Tables 1 and 2 the highest occupied MOs of the most populated guanine tautomers **1** and **2** are characterized by their calculated Mulliken atomic orbital populations (see also Supporting Information). Following these qualitative considerations the MOs are assigned to σ- and π-types orbitals and, when appropriate, to specific combinations of atomic lone pair (LP) orbitals. As follows from comparison of the MOs obtained for planar and fully optimized nonplanar guanine,[24] pyramidalization of the NH_2 group in the latter case can be considered as a small perturbation which basically preserves the character and the energetic ordering of the orbitals, so that the above σ- and π-classification scheme always applies.

Under our experimental conditions, guanine tautomer **2** is expected to be the most populated,[24] and its photoelectron spectrum should therefore to a large extent shape the overall spectral profile of guanine. The results of our ADC(3) and OVGF calculations for tautomer **2** are indeed in good agreement with the synchrotron radiation measurements (Figure 2, Table 3). The ADC(3) spectrum reproduces satisfactorily all major features of the experimental profile, with some differences in intensity for some features. It can be seen that bands A−D between 8 and 12 eV of the experimental spectrum are due to the seven lowest photoelectron transitions. This part of the

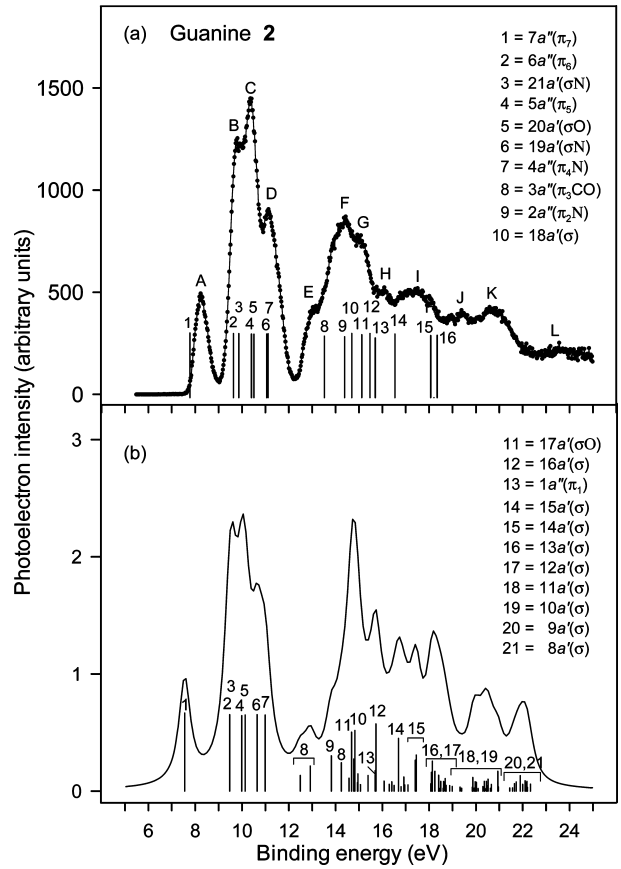

Figure 2. (a) Dotted line: valence shell photoelectron spectrum of guanine, photon energy of 100 eV. Bar spectrum: guanine **2** spectrum calculated using the OVGF approach. (b) Theoretical photoelectron spectrum of guanine **2** obtained using the ADC(3) method.

TABLE 3: Calculated Energies (*E*, eV) and Intensities (*P*) for Outer-Valence Vertical Ionization Transitions in Guanine 2

		6-31G basis[a]					6-311++G** basis				
		HF	OVGF		ADC(3)		OVGF[a]		OVGF[b]		P3[c]
MO	type	*E*	*E*	*P*	*E*	*P*	*E*	*P*	*E*	*P*	*E*
7a″	π_7	8.36	7.40	0.90	7.55	0.89	7.78	0.90	8.03	0.90	8.27
6a″	π_6	10.55	9.28	0.90	9.48	0.87	9.64	0.89	9.79	0.89	9.94
21a′	$\sigma_{LPN3,\ N9,O}$	11.47	9.22	0.90	9.57	0.89	9.87	0.89	10.02	0.89	9.91
5a″	π_5	11.90	9.94	0.89	9.99	0.86	10.40	0.88	10.61	0.88	10.58
20a′	$\sigma_{LPO,N3}$	12.17	10.06	0.89	10.14	0.87	10.51	0.88	10.63	0.88	10.27
19a′	$\sigma_{LPN3,N9}$	12.80	10.39	0.89	10.65	0.87	11.05	0.88	11.22	0.88	11.06
4a″	$\pi_{4\ LPN10,N7}$	12.49	10.78	0.89	10.99	0.87	11.12	0.89	11.29	0.89	11.24
3a″	π_{3CO}	15.17	13.31	0.85	12.49	0.18	13.52	0.85	13.54	0.86	13.29
					12.91	0.29					
					14.25	0.32					
2a″	π_{2LPN7}	16.48	14.17	0.85	13.82	0.40	14.39	0.84	14.41	0.85	14.31
					14.77	0.36					
					15.39	0.18					
18a′	σ	16.64	14.51	0.90	14.83	0.69	14.69	0.89	14.85	0.88	14.77
					14.95	0.20					
17a′	σ_{LPO}	16.90	14.81	0.88	14.68	0.67	15.12	0.87	15.18	0.87	14.91
16a′	σ	17.47	15.32	0.90	15.72	0.77	15.47	0.89	15.58	0.88	15.58
1a″	π_1	18.11	15.59	0.83	15.69	0.23	15.70	0.83	17.92	0.0	15.62
15a″	σ	18.59	16.48	0.89	16.69	0.60	16.54	0.88	16.59	0.88	
					16.91	0.16					
14a′	σ	19.33	17.34	0.89	17.41	0.35	18.07	0.86	35.36	0.0	
					17.45	0.41					
13a′	σ	20.28	17.95	0.88	18.09	0.21	18.21	0.0	19.15	0.0	
					18.14	0.34					
					18.25	0.22					
12a′	σ	20.58	18.24	0.88	18.40	0.18	18.34	0.86	18.35	0.91	

[a] Planar B3LYP/6-311G** geometry (see Supporting Information). [b] Fully optimized MP2/cc-pVTZ geometry.[24] [c] P3 calculations of Dolgounitcheva et al.[6] using 6-311G** basis set.

spectrum is formed by main lines related to the ionization of the highest occupied molecular orbitals, 7a″, 6a″, 21a′, 5a″, 20a′, 19a′.

The next group of bands E−H in the 14−17 eV region comprises transitions related to orbitals 3a″, 2a″, 18a′, 17a′, 16a′, and 1a. This spectral region is more complex since here strong redistribution of spectral intensity from main lines to satellites takes place. The states $(3a'')^{-1}$, $(2a'')^{-1}$, and $(1a'')^{-1}$ of π-symmetry are most strongly involved in this process, and the corresponding one-electron levels are almost entirely missing in the ADC(3) spectrum. It can be seen, for example, that the prominent shoulder E is formed largely by satellites originating from the orbital 3a″(π_3). A similar "selective breakdown effect" was earlier observed for the deep π-orbitals in the other cyclic conjugated compounds.[19]

The spectral bands denoted as I-L are typical "correlation" bands built of the numerous 2h−1p satellites resulting from the breakdown of the molecular orbital picture of ionization for MOs 15a′ and 14a′ (band I), 13a′ and 12a′ (band J), 11a′ and 10a′ (band K) and 9a′ and 8a′ (band L). The relatively large shifts of the ADC(3) predictions with respect to experiment for the inner-valence spectral maxima are within the usual accuracy limits of the ADC(3) method for the satellite states. Since within ADC(3) the 2h−1p configurations are treated less accurately than the main 1h configurations, the absolute accuracy of the ADC(3) calculations generally deteriorates above 13 eV, as the satellite lines begin to dominate in the spectrum. As a result, the assignment of the high-energy maxima is only tentative. Also, one should not forget that the experimental spectrum in fact includes contributions of tautomers **1**, **3**, and **4**, the effect of which is discussed in the following paragraphs.

In Table 3 the present ADC(3)/6-31G calculations are compared with our Hartree−Fock (HF) and OVGF results for basis sets 6-31G and 6-311++G**. Our present OVGF/6-311++G** results and the previous P3 results of Dolgounicheva et al.[6] (both for nonplanar guanine structure) are also included for comparison. Note that the OVGF/TZV results for (planar) guanine **1** and **2** by Jones et al.[8] are essentially identical to the present OVGF/ 6-311++G** results. The experimental (vertical) ionization energies determined as positions of band maxima in the synchrotron radiation spectra are listed in Table 4 together with previous experimental data.[2] As follows from the large energy shifts from HF to OVGF and ADC(3) level of theory, which is especially pronounced for orbitals related to nitrogen lone pairs, the electron correlation and orbital relaxation play important roles in the ionization of guanine. Inversion of orbitals at the OVGF and ADC(3) level relative to the HF picture (e.g., 21a′ and 6a″, 19a′ and 4a″) is further evidence for the importance of electron correlation effects. In agreement with

TABLE 4: Experimental Ionization Energies of Guanine (eV)

band	present[a]	previous[b]
A	8.26	8.28
B	9.81	9.9
C	10.36	10.4
D	11.14	11.2
E	13.05	13.0
F	14.39	
G	15.06	
H	16.09	
I	17.39	
J	19.37	
K	20.71	
L	23.45	

[a] Position of band maxima, as determined from the photoelectron spectra, photon energy 100 eV. [b] Reference 2.

TABLE 5: Calculated Energies (*E*, eV) and Intensities (*P*) for Outer-Valence Vertical Ionization Transitions in Guanine 1

		6-31G basis[a]					6-311++G** basis				
		HF	OVGF		ADC(3)		OVGF[a]		OVGF[b]		P3[c]
MO	type	*E*	*E*	*P*	*E*	*P*	*E*	*P*	*E*	*P*	*E*
7a″	π_7	8.17	7.33	0.90	7.47	0.89	7.67	0.90	8.01	0.90	8.13
21a′	$\sigma_{LPN7,N3,O}$	11.49	9.23	0.90	9.52	0.89	9.86	0.89	10.00	0.89	9.82
6a′	π_6	11.13	9.58	0.89	9.70	0.87	9.94	0.89	10.11	0.89	10.20
20a′	$\sigma_{LPO,N7}$	11.94	9.86	0.88	9.87	0.86	10.24	0.88	10.31	0.88	10.02
5a″	$\pi_{5LPN1,O}$	11.79	9.96	0.89	9.95	0.86	10.37	0.88	10.47	0.88	10.40
4a″	$\pi_{4LPN10,N3}$	12.28	10.52	0.89	10.81	0.85	10.92	0.88	11.12	0.89	11.12
19a′	$\sigma_{LP\ N3,\ N7}$	13.20	10.73	0.89	11.07	0.88	11.43	0.88	11.61	0.88	11.50
3a″	π_{3CO}	15.15	13.26	0.85	12.49	0.33	13.46	0.85	13.49	0.86	13.28
					13.25	0.22					
2a′	π_{2LPN9}	16.43	14.15	0.86	14.23	0.44	14.35	0.85	14.43	0.86	14.35
					14.46	0.53					
18a′	σ	16.57	14.48	0.90	14.88	0.72	14.63	0.89	14.65	0.88	14.62
17a′	σ_{LPO}	16.66	14.53	0.88	14.35	0.69	14.87	0.87	14.94	0.87	14.50
					14.54	0.20					
16a′	σ	17.37	15.18	0.90	15.59	0.74	15.36	0.89	15.41	0.88	15.48
1a″	π_1	18.13	15.58	0.85	15.04	0.26	15.70	0.84	15.84	0.84	15.71
					15.96	0.47					
15a′	σ	18.58	16.30	0.88	16.55	0.61	16.37	0.89	16.50	0.88	
14a′	σ	19.39	17.49	0.90	17.49	0.38	17.66	0.87	17.44	0.89	
					17.57	0.27					
13a′	σ	20.28	17.92	0.88	18.02	0.41	18.05	0.87	17.88	0.88	
12a′	σ	20.44	18.05	0.88	18.37	0.66	18.15	0.87	18.93	0.0	
					18.52	0.21					

[a] Planar B3LYP/6-311G** geometry (see Supporting Information). [b] Fully optimized MP2/cc-pVTZ geometry.[24] [c] P3 calculations of Dolgounitcheva et al.[6] using 6-311G** basis set.

previous observations,[10] the OVGF and ADC(3) results for the outermost MOs in the 6-31G basis set are quite similar to each other and demonstrate only slight improvement at the ADC(3) level. The OVGF and ADC(3) results begin to diverge for deeper orbitals starting from the orbital 3a. This is because the OVGF is unable to treat the situation where intense satellite formation takes place, as is the case in the guanine photoelectron spectrum above 13 eV. The breakdown of the OVGF approximation here is reflected also by zero pole strengths obtained at the 6-311++G** level for the orbitals 1a″, 14a′, and 13a′ and weird ionization energy of 35.36 eV predicted for orbital the 14a′.

As follows from the comparison of the OVGF results for different basis sets, the present theoretical estimates of ionization energies obtained using the 6-31G basis set are subject to improvement. Most of the energies increase by about 0.4 eV when more extended 6-311++G** basis sets are employed. It is interesting to note that for σ-orbitals related to the nitrogen lone pairs even larger energy corrections up to 0.7 eV take place. Since for the same (6-31G) basis set the ADC(3) results are closer to the experimental values than the OVGF results, the above observations allow one to expect that the agreement with experiment could improve significantly if ADC(3) calculations using the 6-311++G** basis set could be performed. This is, however, computationally too expensive at present.

Finally, we note that the use of the fully optimized nonplanar geometries slightly increases ionization energies. The largest energy change of 0.25 eV is observed for the lowest orbital 7a″ and significantly improves the agreement between the presently calculated and measured ionization energies for this orbital (8.03 and 8.26 eV, respectively). The lowest π-orbital in the other guanine tautomers is equally sensitive toward variation of geometrical parameters (Tables 5−7). This implies that the accurate structural calculations are essential for quantitative predictions of ionization energies, but reliable assignments of qualitative level can be obtained already using the planar approximation. The latter justifies the present ADC(3) assignments. The P3/6-311G** calculations of Dolgounicheva et al.[6] for the 7a″ MO are in very good agreement with experimental data but demonstrate no advantage over the present OVGF results for the other MOs. The P3 and OVGF energy difference is not uniform and leads to the opposite order of certain levels, e.g., in the MOs pairs (5a″ and 20a′) and (6a″ and 21a′).

The calculated ionization spectra of guanine tautomers **1**, **3**, and **4** (Figures 3−5, Tables 5−7) have obvious similarities with the spectrum of tautomer **2**. This is a consequence of similarities in the MO structure and presence of common chemical motifs, such as the C−C, O−C, and N−C double bonds, and the oxygen and nitrogen lone pairs (Figure 1). As predicted by the present calculations, the first seven ionization potentials in tautomers **1**, **3**, and **4** occur within the same energy range (7−12 eV) as in tautomer **2**. The distribution of spectral lines and character of certain transitions is, however, different, which leads to individual patterns of the spectral envelopes. In all tautomers, the lowest binding energy transition involves the highest occupied MO 7a″(π_7), associated with the C_4-C_5 π-bond, and is at relatively constant energy and also well separated from the other transitions. The next two transitions 6a″$(\pi_6)^{-1}$ and 21a′$(\sigma_{N,O})^{-1}$ are nearly degenerate. The same is true for the following two transitions 5a″$(\pi_5)^{-1}$ and 20a′$(\sigma_{O,N})^{-1}$ in **1** and **2**, or 20a′$(\sigma_{N,O})^{-1}$ in **3** and **4**. Here we face the situation discussed in our previous studies of uracils[21] and observed in many Green's function nucleic acid base studies:[6,14,15,30] π-orbitals and σ-orbitals of heteroatom lone pairs, being well separated at the HF level, become very close or nearly degenerate in energy at the ADC(3), OVGF, and P3 level of treatment. The actual reason for this is still unclear but in all cases the final states of σ-symmetry experience (on average 1.3−1.4 times) larger shifts when the electron correlation and relaxation effects are taken into account. A similar though less pronounced situation can be observed for 4a″$(\pi_4)^{-1}$ and 19a′$(\sigma_N)^{-1}$ also found in the low-

TABLE 6: Calculated Energies (*E*, eV) and Intensities (*P*) for Outer-Valence Vertical Ionization Transitions in Guanine 3

		6-31G basis[a]					6-311++G** basis				
		HF	OVGF		ADC(3)		OVGF[a]		OVGF[b]		P3[c]
MO	type	*E*	*E*	*P*	*E*	*P*	*E*	*P*	*E*	*P*	*E*
7a″	π_7	8.34	7.51	0.91	7.64	0.89	7.77	0.90	8.07	0.90	8.18
6a″	π_6	10.60	9.16	0.90	9.29	0.88	9.48	0.89	9.60	0.89	9.71
21a′	$\sigma_{LPN3,N1,N7}$	11.19	9.01	0.90	9.36	0.89	9.55	0.89	9.66	0.89	9.63
5a″	$\pi_{5LPN10,O}$	11.89	10.14	0.89	10.23	0.86	10.50	0.88	10.67	0.88	10.57
20a′	$\sigma_{LPN1,N7}$	12.41	10.09	0.89	10.41	0.89	10.64	0.88	10.74	0.88	10.64
4a″	π_4	12.22	10.68	0.89	10.88	0.86	10.95	0.88	10.96	0.88	10.94
19a′	$\sigma_{LPN1,N3,N7}$	13.78	11.34	0.89	11.66	0.87	11.92	0.88	12.00	0.88	11.83
3a″	$\pi_{3LPO,N10}$	15.46	13.41	0.87	13.24	0.38	13.62	0.86	13.62	0.86	13.42
					14.07	0.33					
18a′	σ_{LPO}	15.71	13.59	0.90	13.67	0.89	14.06	0.89	14.16	0.89	13.94
2a″	$\pi_{2LPN9,O}$	16.41	14.19	0.87	14.27	0.65	14.39	0.86	14.48	0.86	14.24
17a′	σ	16.85	14.82	0.90	15.07	0.60	14.92	0.89	14.94	0.89	14.96
					15.12	0.25					
16a′	σ	17.56	15.26	0.89	15.54	0.61	15.29	0.88	15.39	0.89	15.39
					15.68	0.24					
1a″	π_1	18.00	15.56	0.84	15.23	0.22	15.60	0.83	17.78	0.0	
					16.22	0.19					
15a′	σ	17.98	16.02	0.89	16.22	0.81	16.10	0.88	16.01	0.86	
14a′	σ	18.78	16.80	0.89	17.00	0.79	17.07	0.89	16.82	0.90	
13a′	σ	19.54	17.38	0.88	17.53	0.28	17.49	0.84	18.09	0.04	
					17.63	0.25					
					17.65	0.24					

[a] Planar B3LYP/6-311G** geometry (see Supporting Information). [b] Fully optimized MP2/cc-pVTZ geometry.[24] [c] P3 calculations of Dolgounitcheva et al.[6] using 6-311G** basis set.

TABLE 7: Calculated Energies (*E*, eV) and Intensities (*P*) for Outer-Valence Vertical Ionization Transitions in Guanine 4

		6-31G basis[a]					6-311++G** basis				
		HF	OVGF		ADC(3)		OVGF[a]		OVGF[b]		P3[c]
MO	type	*E*	*E*	*P*	*E*	*P*	*E*	*P*	*E*	*P*	*E*
7a″	π_7	8.43	7.54	0.91	7.66	0.89	7.79	0.90	8.09	0.90	8.22
6a″	π_6	10.59	9.17	0.89	9.29	0.88	9.52	0.89	9.63	0.89	9.72
21a′	$\sigma_{LPN1,N3}$	11.14	8.97	0.90	9.33	0.89	9.52	0.89	9.62	0.89	9.57
5a″	$\pi_{5LPN10,O}$	11.90	10.17	0.89	10.29	0.86	10.50	0.88	10.63	0.88	10.52
20a′	$\sigma_{LPN1,N7}$	12.56	10.23	0.89	10.57	0.89	10.76	0.88	10.87	0.88	10.79
4a″	π_4	12.43	10.85	0.89	11.05	0.86	11.09	0.88	11.13	0.88	11.14
19a′	$\sigma_{LPN3,N7}$	13.82	11.36	0.88	11.66	0.87	11.95	0.88	12.04	0.88	11.86
3a″	$\pi_{3LPO,N10}$	15.42	13.38	0.87	13.22	0.40	13.60	0.86	13.61	0.86	13.40
					13.77	0.19					
					14.11	0.31					
18a′	σ_{LPO}	15.57	13.39	0.90	13.50	0.89	13.83	0.89	13.93	0.89	13.74
2a″	$\pi_{2LPN9,O}$	16.45	14.22	0.87	14.30	0.59	14.42	0.86	14.51	0.86	14.25
17a′	σ	17.04	15.00	0.90	15.27	0.81	15.06	0.89	15.08	0.89	15.11
1a″	π_1	18.08	15.62	0.83	15.22	0.19	15.65	0.82	15.89	0.84	
					16.26	0.28					
16a′	σ	17.82	15.95	0.90	16.04	0.81	16.03	0.88	15.92	0.86	15.71
					16.36	0.22					
15a′	σ	18.05	15.95	0.89	16.24	0.35	16.13	0.88	15.93	0.88	
					16.34	0.32					
14a′	σ	18.96	16.64	0.89	16.85	0.25	16.75	0.86	16.96	0.78	
					16.93	0.49					
13a′	σ	19.63	17.49	0.88	17.70	0.40	18.28	0.0	18.32	−0.11	
12a′	σ	20.62	18.50	0.88	18.66	0.55	18.60		18.50	0.87	

[a] Planar B3LYP/6-311G** geometry (see Supporting Information). [b] Fully optimized MP2/cc-pVTZ geometry.[24] [c] P3 calculations of Dolgounitcheva et al.[6] using 6-311G** basis set.

energy spectral region of guanine under consideration. Since the predicted energy separation of the $^2A''(\pi)$ and $^2A''(\sigma)$ final ionic states is small within the pairs, one should not exclude the possibility of vibronic interaction via nontotally symmetric vibrational modes. As is well-known, such vibronic coupling may strongly complicate the appearance and interpretation of the corresponding spectra.[31] For such transitions, it may also be difficult to extract the accurate vertical ionization energies from the experimental data and the interpretation of the spectrum should rely upon adequate theoretical modeling accounting for vibronic effects rather than electronic structure calculations dealing with vertical ionization potentials.

The next part of the spectrum common to all tautomers extends from 13 to approximately 18 eV. Here one finds only few intact main-state lines, which are embedded in a dense satellite structure. Above 20 eV the spectral bands are built

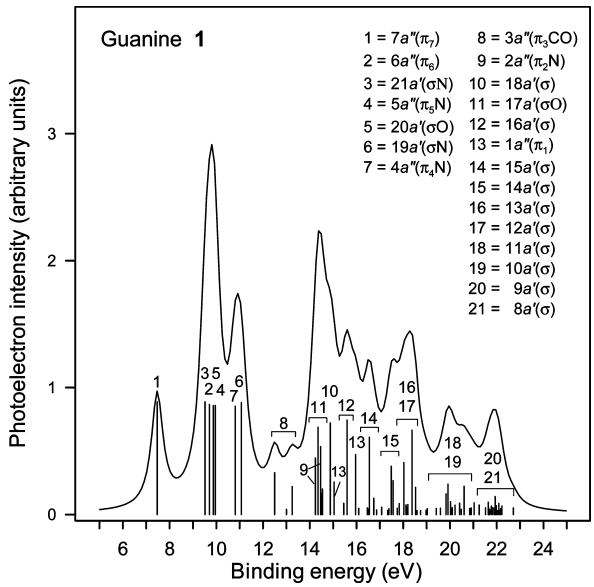

Figure 3. Theoretical photoelectron spectrum of guanine **1** obtained using the ADC(3)/6-31G method.

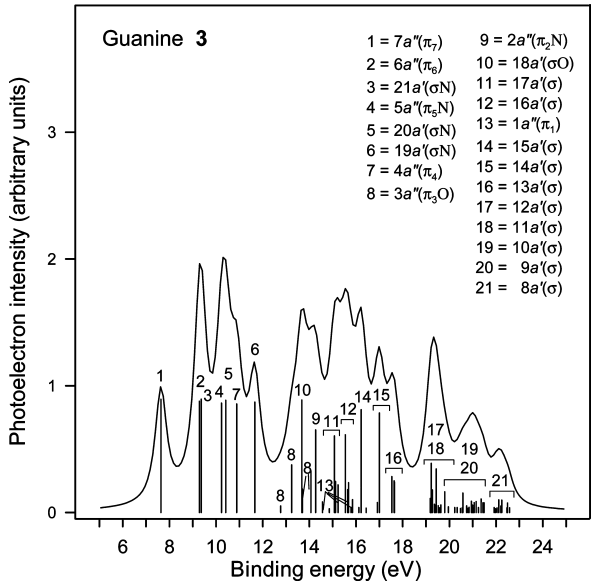

Figure 4. Theoretical photoelectron spectrum of guanine **3** obtained using the ADC(3)/6-31G method.

exclusively of satellites. Such bands are often referred to as "correlation bands". As was already noted for the **2** form of guanine, the innermost π-type MOs of the tautomers **1**, **3**, and **4** are subject to strong intensity redistribution. The shakeup and shake-down satellites arising in the spectra in place of the corresponding one-electron levels are spread between 13 and 18 eV.

As expected, according to our ADC(3) and OVGF results, the outer-valence spectrum of guanine tautomer **3** corresponds closely to the spectrum of tautomer **4**. Since the tautomers **3** and **4** are the OH-rotamers, the main differences in their ionization spectra are due to σ-orbitals with pronounced oxygen character, such as 18a′(σ_{LPO}) and 16a′(σ), Tables 3 and 4. The theoretical spectral envelopes of guanine **3** (Figure 4) and **4** (Figure 5) have much in common. This reflects the similarity of the electronic structure of the two rotational conformers. The spectra differ mainly by the structure above 13 eV, where somewhat different distributions of the main and satellite states give rise to different overall envelopes. As seen from Tables 6 and 7, the vertical ordering of the lowest ionization events in guanine **3** and **4** crucially depends on the quality of theoretical scheme and basis set used in the calculations.

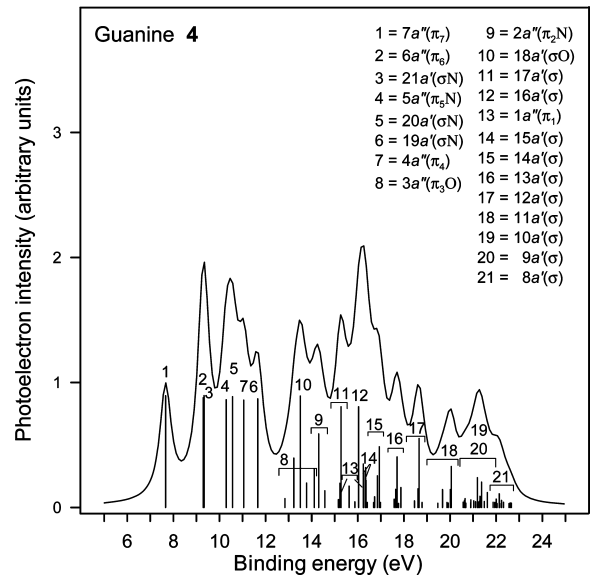

Figure 5. Theoretical photoelectron spectrum of guanine **4** obtained using the ADC(3)/6-31G method.

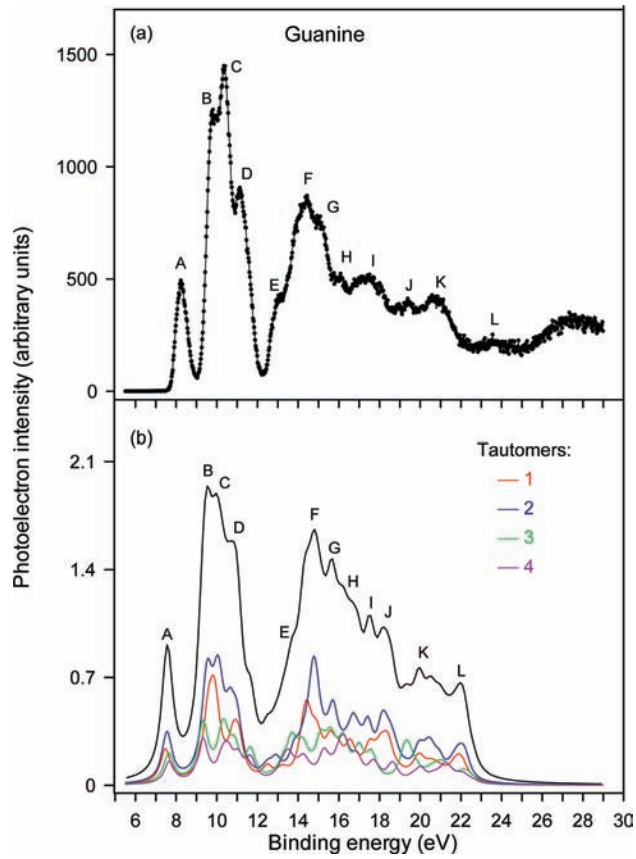

Figure 6. (a) Valence shell photoelectron spectrum of guanine, photon energy 100 eV. (b) Composite theoretical spectrum of guanine, constructed from the Boltzmann-weighted sum for $T = 600$ K of the individual spectra representing the **1**−**4** forms. The individual contributions are also shown.

Finally, in Figure 6 we present the composite theoretical spectrum of guanine constructed as the Boltzmann-weighted sum of the ADC(3)/6-31G spectra of the forms **1**−**4**. The theoretical spectrum is in good qualitative agreement with the experimental

profile. All of the lowest experimental band maxima (A−G) can be unambiguously identified in the theoretical spectrum, and there are only some small shifts in energy, or small differences in intensity. The assignment of the maxima H−M is less straightforward as the theoretical profile in the corresponding region reproduces the experimental spectrum less accurately, for reasons explained above. As follows from the analysis of the individual contributions, also shown in Figure 6, the theoretical spectral envelope is shaped mainly by the spectra of forms **2** and **1**. The contributions of the forms **3** and **4** are also important, but since their band positions above 13 eV are rather different from those of forms **1** and **2**, they mainly smooth the spectrum in this energy region.

IV. Conclusions

The inner and outer valence band photoionization spectra of four tautomers of guanine have been investigated theoretically and compared with the experimental spectrum. The spectrum calculated from a Boltzmann weighted sum of individual spectra is in good agreement with theory. The features have been assigned and the character of the valence states reported. The data do not show features that can be traced unambiguously to a particular tautomer. The lower energy part of the spectrum is dominated by single hole states, while the higher energy part is dominated by multielectron excitations, as observed for other heterocyclic compounds.

Acknowledgment. Part of the present theoretical results for guanine were obtained and discussed in the course of our previous work[14] in collaboration with D. M. P. Holland. The theoretical part of this study was supported by a grant of the Russian Foundation for Basic Research (RFBR). O.P. acknowledges financial support from the Area di Ricerca di Trieste under the Incoming Mobility scheme.

Supporting Information Available: Complete ref 26, ground-state geometries of guanine tautomers (Figure 1) optimized in the approximation of planar molecular structures at the DFT B3LYP/6-311G** level of theory, Mulliken atomic population in the outer-valence molecular orbitals of guanine tautomers **1**−**4** calculated at the HF/6-31G level of theory. This material is available free of charge via the Internet at http://pubs.acs.org.

References and Notes

(1) Choi, M. Y.; Miller, R. E. *J. Am. Chem. Soc.* **2006**, *128*, 7320, and references therein.

(2) Lin, J.; Yu, C.; Peng, S.; Akiyama, I.; Li, K.; Lee, L. K.; LeBreton, P. R. *J. Phys. Chem.* **1980**, *84*, 1006.

(3) Dougherty, D.; Younathan, E. S.; Voll, R.; Abdulnur, S.; McGlynn, S. P. *J. Electron Spectrosc. Relat. Phenom.* **1978**, *13*, 379.

(4) Hush, N. S.; Cheung, A. S. *Chem. Phys. Lett.* **1975**, *34*, 11.

(5) Dougherty, D.; McGlynn, S. P. *J. Chem. Phys.* **1977**, *67*, 1289.

(6) Dolgounitcheva, O.; Zakrzewski, V. G.; Ortiz, J. V. *J. Am. Chem. Soc.* **2000**, *122*, 12304.

(7) (a) Ortiz, J. V. *J. Chem. Phys.* **1996**, *104*, 7599. (b) Ferreira, A. M.; Seabra, G.; Dolgounitcheva, O.; Zakrzewski, V. G.; Ortiz, J. V. In *Quantum-Mechanical Prediction of Thermochemical Data*; Cioslowski, J., Ed.; Kluwer: Dordrecht, The Netherlands, 2001.

(8) (a) Jones, D. B.; Wang, F.; Winkler, D. A.; Brunger, M. J. *Biophys. Chem.* **2006**, *121*, 105. (b) Jones, D. B.; Wang, F.; Winkler, D. A.; Brunger, M. J. *Biophys. Chem.* **2007**, *125*, 560.

(9) (a) Gritsenko, O. V.; van Leeuwen, R.; Baerends, E. J. J. *Chem. Phys.* **1994**, *101*, 8955. (b) Gritsenko, O. V.; van Leeuwen, R.; Baerends, E. J. *Phys. Rev. A* **1995**, *52*, 1870. (c) Gritsenko, O. V.; Schipper, P. R. T.; Baerends, E. J. *Chem. Phys. Lett.* **1999**, *302*, 199.

(10) von Niessen, W.; Schirmer, J.; Cederbaum, L. S. *Comput. Phys. Rep.* **1984**, *1*, 57.

(11) (a) Zakrzewski, V. G.; von Niessen, W. *J. Comput. Chem.* **1993**, *14*, 13. (b) Zakrzewski, V. G.; Ortiz, J. V. *Int. J. Quantum Chem.* **1995**, *53*, 583. (c) Zakrzewski, V. G.; Ortiz, J. V. *Int. J. Quantum Chem.* **1994**, *S28*, 23.

(12) Schirmer, J.; Cederbaum, L. S.; Walter, O. *Phys. Rev. A* **1983**, *28*, 1237.

(13) Schirmer, J.; Angonoa, G. *J. Chem. Phys.* **1989**, *91*, 1754.

(14) Trofimov, A. B.; Schirmer, J.; Kobychev, V. B.; Potts, A. W.; D.; Holland, M. P.; Karlsson, L. *J. Phys. B: At. Mol. Opt. Phys.* **2006**, *39*, 305.

(15) Potts, A. W.; Holland, D. M. P.; Trofimov, A. B.; Schirmer, J.; Karlsson, L.; Siegbahn, K. *J. Phys. B: At. Mol. Opt. Phys.* **2003**, *36*, 3129.

(16) Cederbaum, L. S.; Domcke, W.; Schirmer, J.; von Niessen, W. *Adv. Chem. Phys.* **1986**, *65*, 115.

(17) Mertins, F.; Schirmer, J. *Phys. Rev. A* **1996**, *53*, 2140.

(18) Schirmer, J.; Mertins, F. *Int. J. Quantum Chem.* **1996**, *58*, 329.

(19) (a) Trofimov, A. B.; Schirmer, J.; Holland, D. M. P.; Karlsson, L.; Maripuu, R.; Siegbahn, K.; Potts, A. W. *Chem. Phys.* **2001**, *263*, 167. (b) Potts, A. W.; Trofimov, A. B.; Schirmer, J.; Holland, D. M. P.; Karlsson, L. *Chem. Phys.* **2001**, *271*, 337. (c) Trofimov, A. B.; Schirmer, J.; Holland, D. M. P.; Potts, A. W.; Karlsson, L.; Maripuu, R.; Siegbahn, K. *J. Phys. B: At. Mol. Opt. Phys.* **2002**, *35*, 5051. (d) Powis, I.; Zaytseva, I. L.; Trofimov, A. B.; Schirmer, J.; Holland, D. M. P.; Potts, A. W.; Karlsson, L. *J. Phys. B: At. Mol. Opt. Phys.* **2007**, *40*, 2019. (e) Trofimov, A. B.; Zaytseva, I. L.; Moskovskaya, T. E.; Vitkovskaya, N. M. *Chem. Heterocycl. Compd.* **2008**, *44*, 1101.

(20) (a) Deleuze, M. S.; Trofimov, A. B.; Cederbaum, L. S. *J. Chem. Phys.* **2001**, *115*, 5859. (b) Deleuze, M. S. *J. Chem. Phys.* **2002**, *116*, 7012. (c) Deleuze, M. S. *J. Phys. Chem. A* **2004**, *108*, 9244. (d) Deleuze, M. S.; Claes, L.; Kryachko, E. S.; François, J.-P. *J. Chem. Phys.* **2003**, *119*, 3106.

(21) (a) Holland, D. M. P.; Potts, A. W.; Karlsson, L.; Zaytseva, I. L.; Trofimov, A. B.; Schirmer, *J. Chem. Phys.* **2008**, *352*, 205. (b) Holland, D. M. P.; Potts, A. W.; Karlsson, L.; Zaytseva, I. L.; Trofimov, A. B.; Schirmer, *J. Chem. Phys.* **2008**, *353*, 47.

(22) Hehre, W. J.; Ditchfield, R.; Pople, J. A. *J. Chem. Phys.* **1972**, *56*, 2257.

(23) Krishnan, R.; Binkley, J. S.; Seeger, R.; Pople, J. A. *Chem. Phys.* **1980**, *72*, 650.

(24) Plekan, O.; Feyer, V.; Richter, R.; Coreno, M.; Vall llosera, G.; Prince, K. C.; Trofimov, A. B.; Zaytseva, I. L.; Moskovskaya, T. E.; Gromov, E. V.; Schirmer, J. *J. Phys. Chem. A* **2009**, *113*, 9376.

(25) (a) Becke, A. D. *J. Chem. Phys.* **1993**, *98*, 5648. (b) Lee, C.; Yang, W.; Parr, R. G. *Phys. Rev. B* **1988**, *37*, 785.

(26) Frisch, M. J.; et al. *Gaussian 98*, revision A.7; Gaussian, Inc.: Pittsburgh, PA, 1998.

(27) The ADC(3) code originally written by G. Angonoa, O. Walter and J. Schirmer; further developed by M. K. Scheller and A. B. Trofimov.

(28) Schmidt, M. W.; Baldridge, K. K.; Boatz, J. A.; Elbert, S. T.; Gordon, M. S.; Jensen, J. H.; Koseki, S.; Matsunaga, N.; Nguyen, K. A.; Su, S.; Windus, T. L.; Dupuis, M.; Montgomery, J. A., Jr. *J. Comput. Chem.* **1993**, *14*, 1347.

(29) Prince, K. C.; Blyth, R. R.; Delaunay, R.; Zitnik, M.; Krempasky, J.; Slezak, J.; Camilloni, R.; Avaldi, L.; Coreno, M.; Stefani, G.; Furlani, C.; de Simone, M.; Stranges, S. *J. Synchrotron Radiat.* **1998**, *5*, 565.

(30) Dolgounitcheva, O.; Zakrzewski, V. G.; Ortiz, J. V. *Int. J. Quantum Chem.* **2000**, *80*, 831.

(31) Köppel, H.; Domcke, W.; Cederbaum, L. S. *Adv. Chem. Phys.* **1984**, *57*, 59.

JP905299Z